Ermittlung der turbulenten kinetischen Energiedissipationsrate mittels eines Highspeed-PIV-Experiments mit zwei Kameras

Estimation of turbulent kinetic energy dissipation rate using a two-camera high-speed PIV set-up

Sophie Rüttinger, Marko Hoffmann, Michael Schlüter
Institut für Mehrphasenströmungen, Technische Universität Hamburg-Harburg,
Eißendorfer Straße 38, 21073 Hamburg

Energiedissipationsrate, PIV, Turbulenz
Energy dissipation rate, PIV, turbulence

Summary

In many industrial applications, the turbulent kinetic energy dissipation rate ε is an important criterion for the characterization of the flow structure. The variable ε can be estimated by using the spatial velocity gradients from Particle Image Velocimetry (PIV) measurements. Measurements are conducted with two high-speed cameras, allowing a comparably large field of view with low spatial resolution and a smaller field of view inside with higher spatial resolution. The experimental set-up is presented and results of PIV measurements are shown exemplarily for a turbulent pipe flow behind a Periodic Open Cell Structure (POCS) which is used to generate anisotropic turbulence. The results obtained simultaneously with the two cameras are compared concerning the velocity fields and ε. As correction method for the estimation of ε from PIV data with a lower spatial resolution, the Smagorinsky approach is introduced.
It turns out that the Smagorinsky approach shifts the low resolution results closer to the high resolution results and that the high resolution results are not changed significantly. Thus, it is shown quantitatively that the Smagorinsky approach is suitable to estimate the turbulent kinetic energy dissipation rate from PIV data. Furthermore, the flow structure directly behind the POCS is characterized in detail which will enable in-depth analysis of reactive multiphase flows in future.

Introduction

The knowledge of the turbulent kinetic energy dissipation rate ε, which is the conversion of turbulent kinetic energy into heat per unit of mass and of time, is crucial to design and optimize industrial processes. Examples are mixing processes, chemical reactions and bio processes in stirred vessels or bubble column reactors. In many cases, there is only one value for ε wanted. But when it comes to local phenomena and detailed investigations of flow structures, the knowledge of the distribution of ε can yield further information.
2D PIV measurements provide insight into two velocity components of the velocity vector, and four components of the velocity gradient tensor. Utilizing the spatial velocity gradients, ε can be calculated from its definition. Former research (de Jong et al., 2009) has shown that the results for ε are dependent on the spatial resolution of the experimental set-up. Therefore, in this work, the influence of spatial resolution is analysed. By using an experimental

set-up with two cameras and two objectives, two different spatial resolutions are realized. While the resolution achieved with one camera is a ‘typical’ PIV resolution, the other one is much higher due to a long distance microscope objective. The Smagorinsky approach is a method to deal with the limitation of spatial resolution of most PIV datasets. In this work, it is used to compare the both spatial resolutions obtained with the two cameras.
From the balance of turbulent kinetic energy (Hinze, 1975), the turbulent kinetic energy (TKE) dissipation rate is:

$$\varepsilon = \frac{\nu}{2}\overline{\left(\frac{\partial u_i'}{\partial x_j} + \frac{\partial u_j'}{\partial x_i}\right)^2} \quad (1)$$

Here, ν is the kinematic viscosity and the Einstein notation is utilized. A bar means temporal average. Equation (1) is a sum of 12 summands. Isotropy cannot be assumed for this set-up. But since the cross section of the duct is of square shape, the assumption of symmetry is in order. From this, it follows for the velocities and velocity gradients:

$$u_3' \approx u_1' \, , \quad (2)$$

$$\frac{\partial}{\partial x_3} \approx \frac{\partial}{\partial x_1} \, . \quad (3)$$

Equation (1) then becomes

$$\varepsilon = \nu \cdot \left(8\overline{\left(\frac{\partial u_1'}{\partial x_1}\right)^2} + 2\overline{\left(\frac{\partial u_2'}{\partial x_2}\right)^2} + 2\overline{\left(\frac{\partial u_1'}{\partial x_2}\right)^2} + 2\overline{\left(\frac{\partial u_2'}{\partial x_1}\right)^2} + 4\overline{\left(\frac{\partial u_1'}{\partial x_2}\frac{\partial u_2'}{\partial x_1}\right)}\right). \quad (4)$$

The Smagorinsky approach takes into account that mostly the spatial resolution of PIV measurements is too low to get reliable results. It is known from Large Eddy Simulations in computational fluid dynamics. Assuming a dynamic equilibrium, only the resolved information is needed to estimate the subgrid-scale dissipation. The equation is as follows:

$$\varepsilon \approx \varepsilon_{SGS} = (C_S\Delta)^2\,\overline{\left(\frac{1}{2}\left(\frac{\partial u_i'}{\partial x_j} + \frac{\partial u_j'}{\partial x_i}\right)^2\right)^{\frac{3}{2}}} \quad (5)$$

Here, C_S is the Smagorinsky constant (depending on the velocity gradient calculation method and the window overlap (Bertens et al., 2015)), and Δ is the window size of the PIV data processing.

Experimental Set-up and Procedure

2D high-speed PIV measurements are conducted in a duct made from acrylic glass with a square-shaped cross section which has an edge length of 3 cm. The length of the duct is 0.25 m. The POCS is located at the inflow of the duct and has a mesh size of 3 mm. Demineralized water (T=22°C) is supplied through the duct with a superficial liquid velocity of approximately 0.23 m/s. The PIV seeding is carried out using monodispersed polystyrene particles (MicroParticles GmbH) with a diameter of 3.16 µm and a fluorescence coating.
A Quantronix Darwin Duo Nd:YLF laser (pulse energy approximately 7 mJ per pulse at wavelength of 532 nm) is used (PIV equipment acquired from Intelligent Laser Applications GmbH, Germany). Images of the tracer particles are acquired by a PCO Dimax HS2 at a resolution of 1400 x 1050 pixels^2 (12 bit CMOS) synchronized with the laser at 4 kHz frame rate. While this camera records the whole field of vision (spatial resolution 0.53 mm), a second camera (PCO Dimax HS4) is connected to a long distance microscope (Infinity

K2DistaMax) with only a very small field of view, but a higher spatial resolution (0.1 mm). Detailed information about the experimental set-up can be learned from Figure 1.

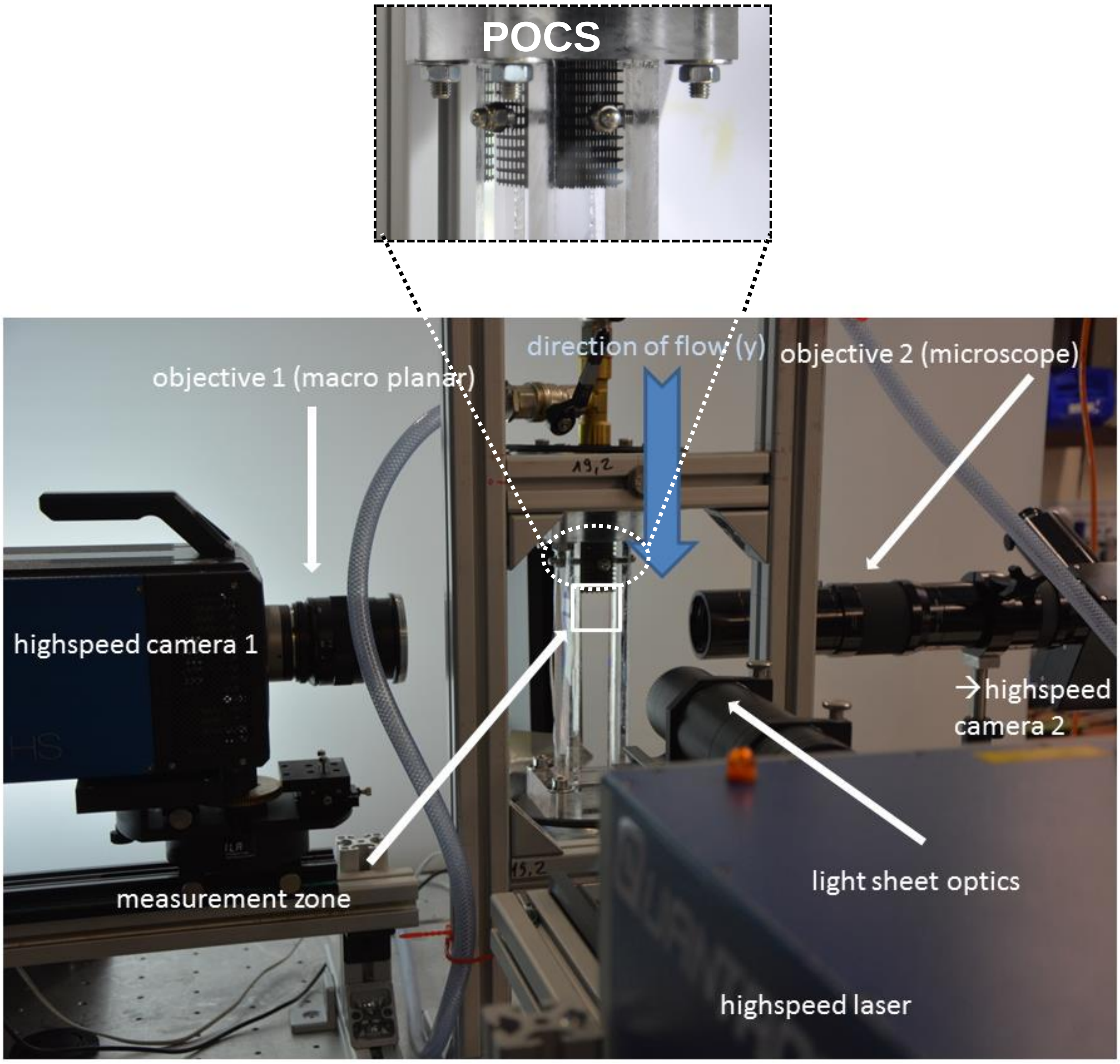

Fig. 1: Experimental set-up.

PIV data processing is carried out using a software (PivView, ILA_5150 GmbH/ PivTec GmbH) with cross-correlation between sequenced images. Window sizes of 48 x 48 pixels^2 are chosen for camera 1, and 32 x 32 pixels^2 for camera 2. 8000 images are processed.

Results and Discussion

The velocity field directly behind the POCS is shown in Figures 2 and 3. Figure 2 depicts the velocity field recorded with camera 1 (lower resolution), while Figure 3 depicts the horizontal velocity profiles. The field of view of camera 2 is also highlighted in Figure 1. The creation of interacting jets due to the POCS is clearly visible. The influence of the POCS is therefore expected to be highest for the vertical positions y_1 and y_2. The vertical positions y_3 and y_4 are within the viewing fields of both cameras.

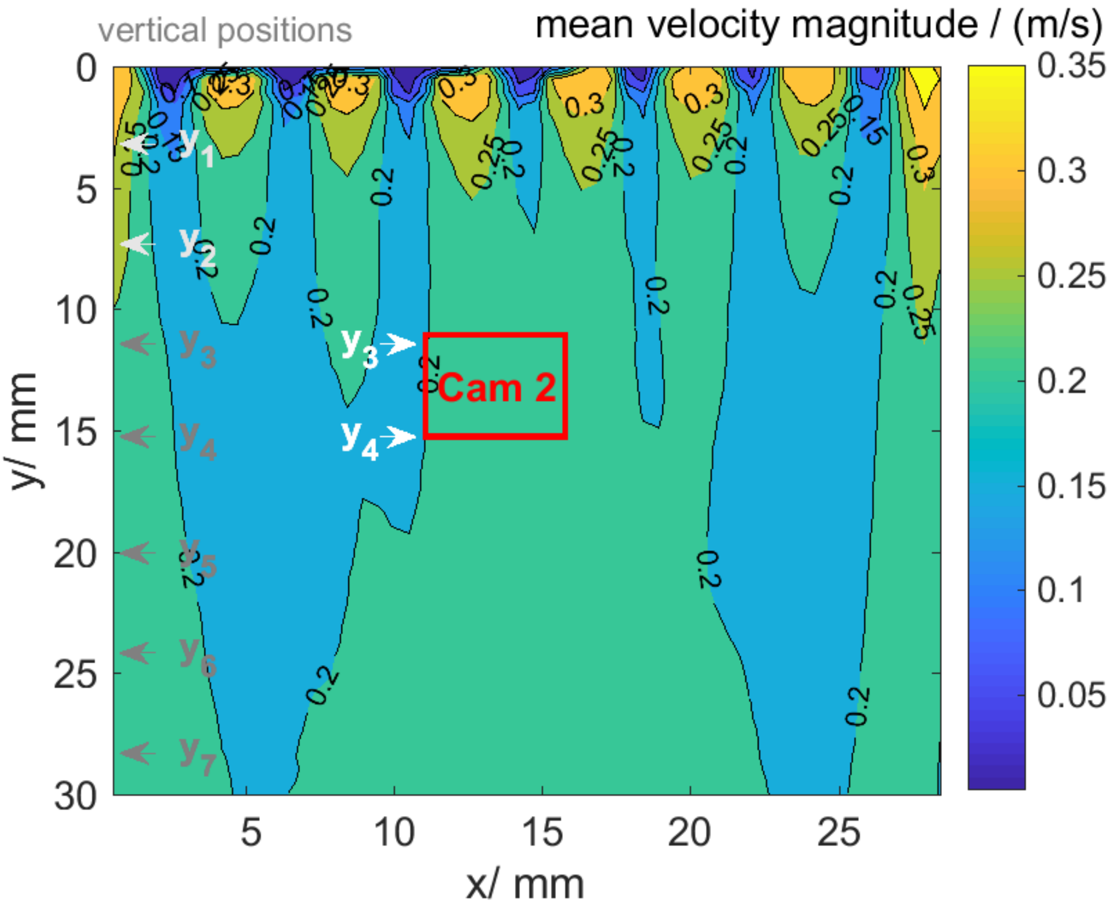

Fig. 2: Velocity field recorded with camera 1.

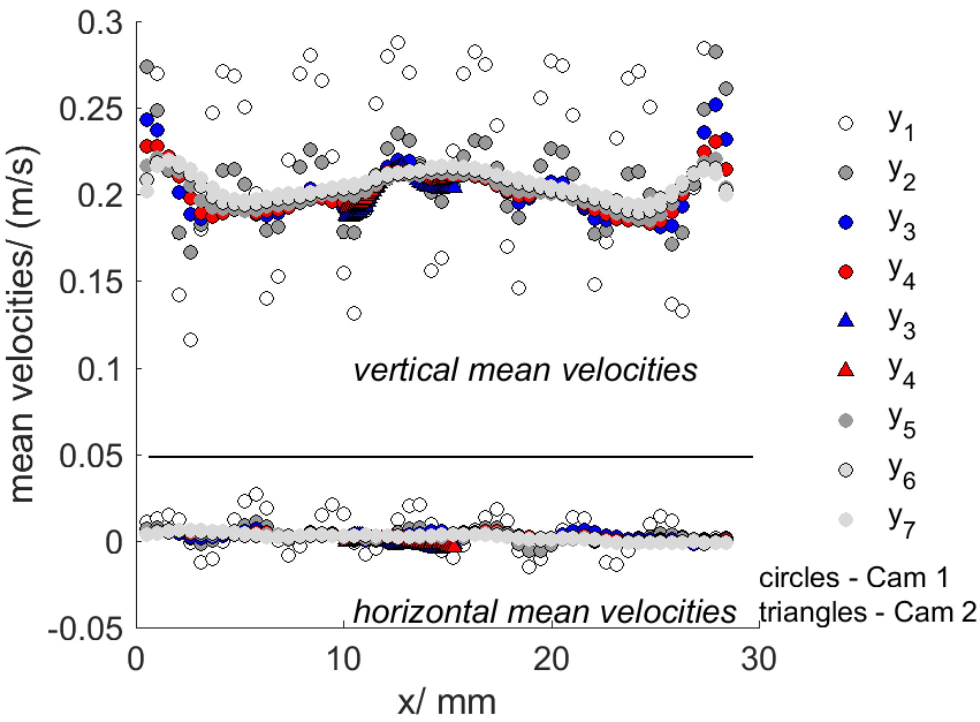

Fig. 3: Velocity profiles.

The TKE is defined as follows

$$k = \frac{1}{3}\left(2 \cdot \overline{u_1{}'u_1{}'} + \overline{u_2{}'u_2{}'}\right). \tag{6}$$

Hereby, the assumption of symmetry is already included. The results for the TKE at the 7 different vertical positions can be taken from Figure 4. The circles depict the TKE profiles which are obtained from the measurements with camera 1, the triangles depict the TKE profiles which are obtained from the measurements with camera 2. It is visible that closer to the POCS, the TKE is higher and fluctuates more. The camera 2 results concerning the TKE are much higher than the camera 1 results. Due to the higher resolution, the velocity fluctuations are also higher. The root mean square velocities are in the range of 0.01 to 0.07 m/s. The decay of the TKE with increasing distance from the POCS is illustrated in Figure 5. For this, the average over all x values is taken and a vertical profile is obtained. The well-known grid turbulence power law (Comte-Bellot and Corrsin, 1966, Mohammed and LaRue, 1990, Pope, 2000) for the TKE is:

$$k = u_{mean}^2\, A \left(\frac{x}{M}\right)^{-n}. \tag{7}$$

To obtain a mean flow velocity u_{mean}, the velocity magnitude is averaged over the whole field of view of camera 1, which leads to a value of 0.18 m/s. M depicts the mesh size of the POCS which is 3 mm. This leads after a curve fitting procedure to the geometry coefficient *A* of 7.5 * 10^{-5} and to a decay coefficient of 0.86.

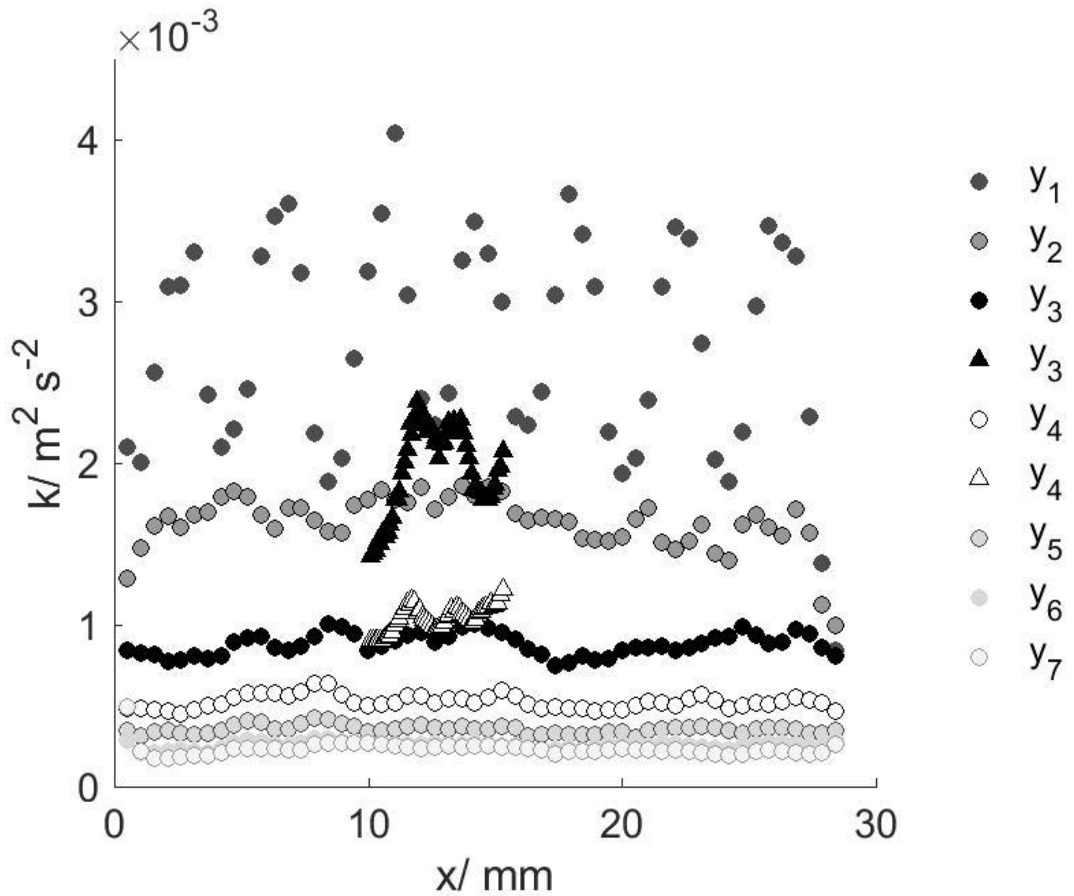

Fig. 4: Turbulent kinetic energy at different vertical positions.

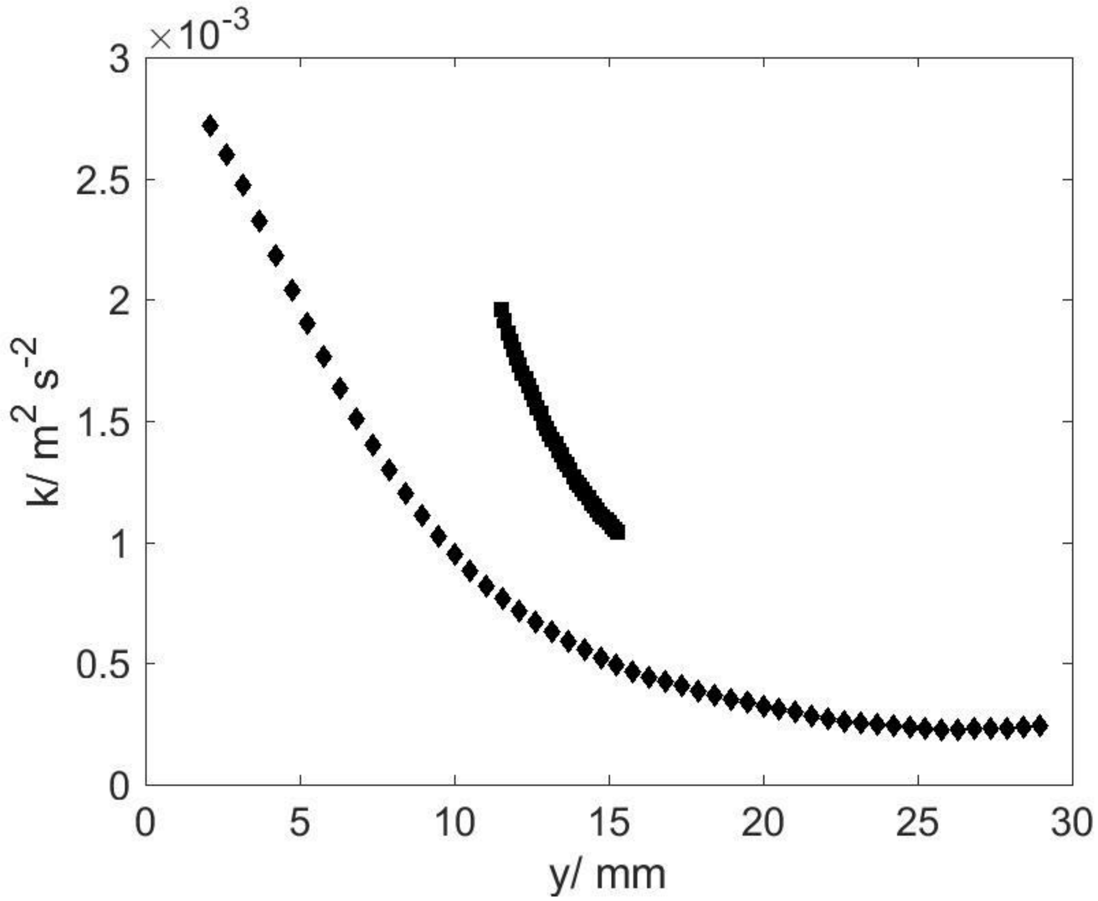

Fig. 5: Decay of TKE from y_1 (3 mm below the POCS) to y_7 (27 mm below the POCS).

The results for ε are presented in Figures 6 and 7. While Figure 6 depicts the uncorrected results using equation (4), Figure 7 depicts the results obtained using the Smagorinsky approach (equation (5)). In both Figures, the decay of ε is clearly visible. It is also visible that the results obtained with camera 2) are much higher than those obtained with camera 1. In general, the Smagorinsky approach leads to higher values for ε and brings the results closer together. But they still differ from each other. By using a dimensional analysis approach, a rough value for the energy dissipation can be estimated:

$$\varepsilon = \frac{\overline{v'^3}}{L} \tag{8}$$

Here, $\overline{v'^3}$ is the fluctuation velocity in the direction of flow, and L is a characteristic length, for which the grid size of the POCS (3 mm) is chosen. This leads to a value for ε of 0.01 m^2/s^3. From the definition of the Kolmogorov scale

$$\eta_K = \left(\frac{\nu^3}{\varepsilon}\right)^{1/4} , \tag{9}$$

a Kolmogorov length of 100 μm is calculated. This is an approach to explain the significant differences even after the Smagorinsky approach. If the smallest scales are in the range mentioned above, than the resolution of camera 2 already meets this scales. In this case, the Smagorinsky approach may not be used since the cut-off wave length should be within the intertial subrange.

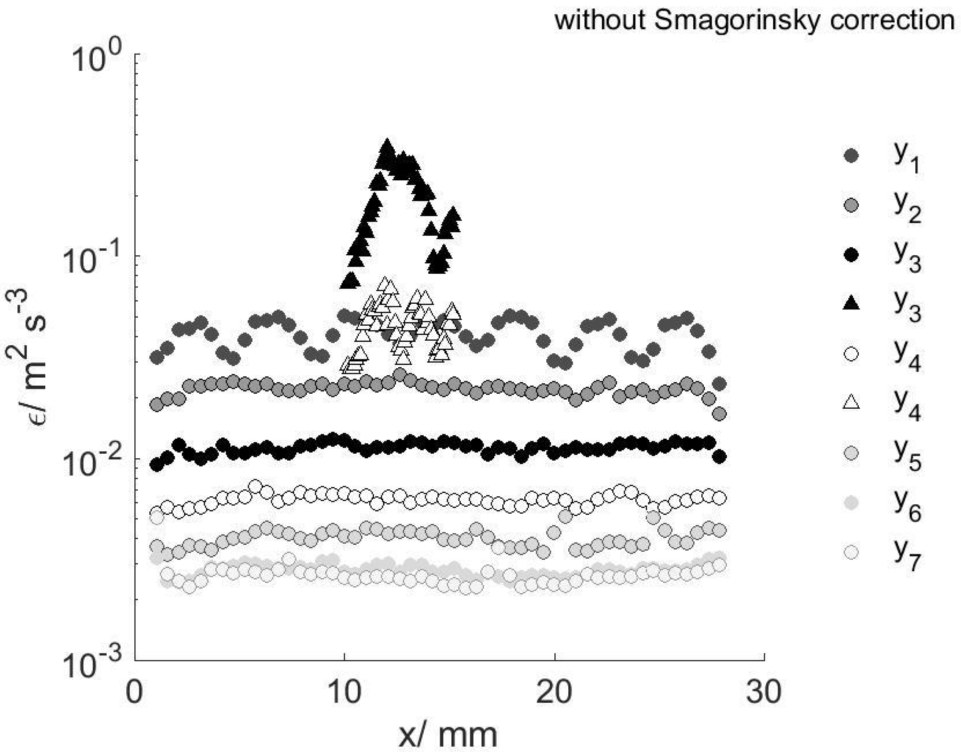

Fig. 6: Energy dissipation rate at different vertical positions.

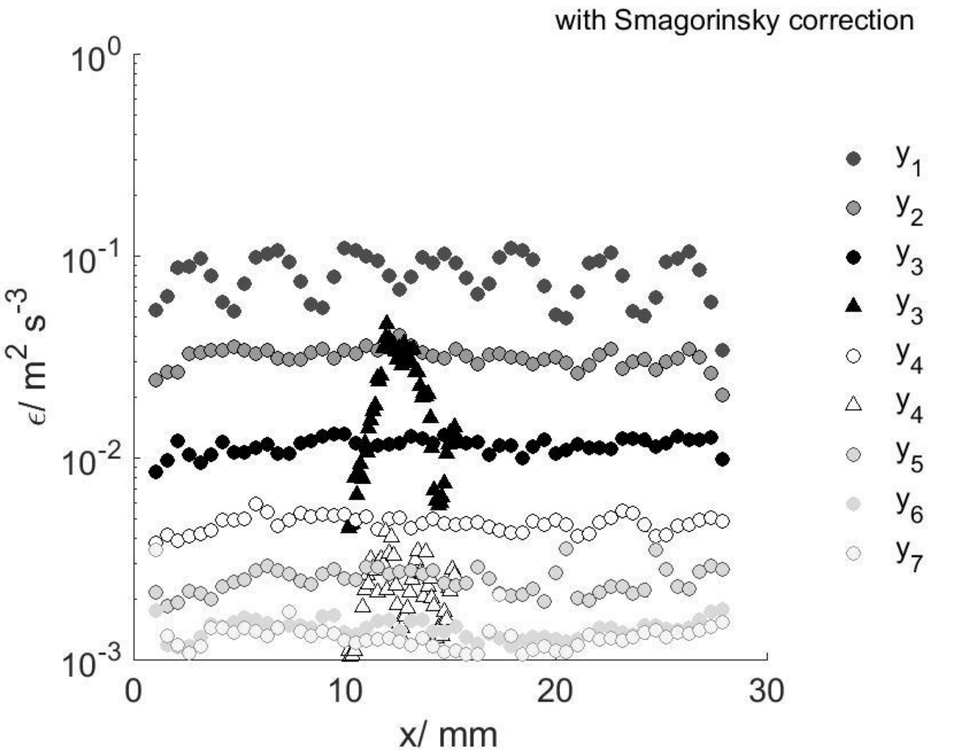

Fig. 7: Energy dissipation rate with Smagorinsky approach at different vertical positions.

Conclusion

In this work, a turbulent flow case behind a 3D grid structure is investigated. The velocity vector fields show interacting jets due to the grid. A decay power law for TKE is applied successfully. To investigate the influence of spatial resolution of PIV measurements on the TKE dissipation rate calculations, two cameras with different spatial resolutions are used. While one camera meets the criterion given by Saarenrinne and Piirto (2000), the other camera does not. As expected, significantly different results for ε are obtained. A correction method (Smagorinsky approach) is used to overcome this issue. It leads to results which lie much closer together and are also very close to an integral estimation. In conclusion, the Smagorinsky approach is suitable to estimate the TKE dissipation rate from PIV datasets with a standard spatial resolution.

Acknowledgements

The authors gratefully acknowledge the support which was given by the Deutsche Forschungsgemeinschaft (DFG) within the priority program SPP1740 under grant number SCHL 617/12-2. The authors want to thank Nicole Grove and PD Dr.-Ing. Yan Jin.

Literature

Bertens, G., van der Hoort, D., Bocanegra-Evans, H., van de Water, W., 2015: “Large‐ eddy estimate of the turbulent dissipation rate using PIV”, Exp Fluids 56, 89.

Comte-Bellot, G., Corrsin, S., 1966: “The use of a contraction to improve the isotropy of grid-generated turbulence”, J Fluid Mech. 25,657.

Hinze, J. O., 1975: "Turbulence", 2nd edition, McGraw-Hill, Inc.

de Jong, J., Cao, L., Woodward, S. H., 2009: "Dissipation rate estimation from PIV in zero-mean isotropic turbulence", Exp. Fluids, 46, 499.

Mohamed, M. S., LaRue, J. C., 1990: “The decay-power law in grid generated turbulence”, J. Fluid Mech. 219, 195.

Pope, S. B., 2000: “Turbulent Flows”, Cambridge University Press.

Saarenrinne, P., Piirto, M., 2000: “Turbulent kinetic energy dissipation rate estimation from PIV velocity vector fields“, Exp. Fluids Supplement S300.